# Yellowknife Cold Climate Heat Pump Study

Mini Split System - Final Report


**To Mark Heyck & Bilal Malik**
**Arctic Energy Alliance**
**5102 51 St #101,**
**Yellowknife, NT X1A 1S7**

**Submitted March 26, 2026 by**
**RDH Building Science Inc.**
**4333 Still Creek Drive**
**Burnaby, BC V5C 6S6**

# Contents

# 1 Introduction

Heat pump systems have been known to deliver 1.5 to 3 times more heat energy than the electrical energy they consume, with efficiency impacted by ambient outdoor air temperatures. Because there is limited research on how this equipment functions in service, particularly in cold climates, it is difficult to predict the true efficiency of air-source heat pumps.

**This research helps to provide a better indication of the energy savings potential and general feasibility of ductless mini split heat pump retrofits in existing homes in Yellowknife, Northwest Territories.** The main objective of this study is to measure cold climate heat pump performance in terms of energy delivered (heating and cooling) and coefficient of performance (COP) against outdoor ambient temperatures. A secondary objective is to understand the seasonal performance COP of these systems compared to published data. A tertiary objective is to understand the amount of heating delivered by a 'control' case using hydronic baseboards relative to the heat pump heating installations.

Cold climate ductless mini split heat pumps were installed in two units of a residential 8-plex. An oil/biomass boiler and hydronic baseboard system was originally the main heating source for all eight units, with HRVs offsetting some of the ventilation heating demand. The hydronic baseboards remain as the primary heating source for the six units without heat pumps, whereas baseboards in the two units with heat pumps are reserved as supplemental heating, to be initiated either when outdoor temperatures are below -30˚C or when the heat pump alone cannot meet the interior set point. Energy delivered by the hydronic baseboards and pre-heating with in-suite HRVs are sub-metered for the two units retrofitted with heat pumps, and in one unit with only baseboards and an HRV (i.e. the control unit). In-situ measurements of key heat pump system and hydronic heating parameters, and corresponding outdoor environment conditions are collected at 5-minute intervals.

Two interim reports were produced previously: for the first six months of the study period (December 1, 2022 to May 31, 2023), and then the following thirteen months (May 1, 2023 to May 31, 2024). On April 20, 2023, an incorrect AC adaptor was replaced with the correct 4.5V model. Seeing as data before this date is considered unreliable, this final report includes findings for the 20-month monitoring period from May 1, 2023 through December 31, 2024.

# 2 Methodology

The methodology for this project was designed in accordance with the International Performance Measurement and Verification Protocol (IPMVP) core concepts (Volume I EVO 10000 – 1:2022).[1] This study uses *Option A: Retrofit Isolation: Key Parameter Measurement* to estimate heat pump efficiency. The main objectives are listed below based on in-situ field performance:

- → Estimate whole house heating and cooling loads from participant utility bill data or energy audit information (if available) – *Note that utility bill data was not available*
- → Estimate heat pump system electrical consumption and external heating element (i.e. electric resistance heating in defrost mode) if applicable
- → Estimate heat delivered by hydronic baseboards and HRV pre-heating
- → Evaluate the impact of outdoor operating temperatures on system performance

## 2.1 Site & System Selection

Two cold climate ductless mini split heat pumps were installed in two units of a residential 8-plex located at 2037 Sissons Court in Yellowknife, Northwest Territories. Yellowknife is in Canada's Sub-Arctic region, situated on the north shore of Great Slave Lake. Throughout an average heating season, Yellowknife experiences roughly 8,000 heating degree days (HDD18.3˚C).[2] Figure 2.1 shows the approximate location of Yellowknife (star) on a map of Canada.


*Figure 2.1 – City of Yellowknife (star) on a map of Canada. Source: Google Maps.*

For this study, Mitsubishi 9,000 BTU/h wall-mounted mini split heat pumps (MSZ-FS09NA-U1 & MUZ-FS09NAH-U1) were installed as retrofits intended to be the new primary heating source for two of the eight units (Units A & C). The published outdoor operating

[1] https://evo-world.org/en/products-services-mainmenu-en/protocols/ipmvp
[2] ASHRAE 2021. ASHRAE Handbook – Fundamentals. American Society of Heating, Refrigerant and Air Conditioning Engineers, Atlanta, GA.

temperature range for heating with these heat pumps is -25˚C to 24˚C,[3] though based on discussions with the manufacturer, there is an understanding that the technology can operate down to -30˚C.

An oil/biomass boiler that supplied the hydronic system (baseboard) and HRV were originally the main heating source for all eight units. The hydronic baseboards remain as the primary heating source for the six units without heat pumps. For Units A & C with the heat pumps, the baseboards are reserved as supplemental heating, to be initiated either when the outdoor temperature is below -30˚C or when the heat pump alone cannot meet the interior set point. Energy delivered by the baseboards and pre-heating by the in-suite HRVs are sub-metered for the two units with heat pumps. One of the units with only baseboards and HRV (Unit B) was also sub-metered as the control unit.

## 2.2 Field Data Collection

This section describes the variables that were measured in the field to estimate the in-situ performance of the heat pumps. The monitoring equipment used to measure the variables discussed in this section was all connected wirelessly to a Linux-based data acquisition gateway with a cellular modem that collected and transferred data to a cloud-based server to facilitate remote access to the monitoring data.

### *System and Fan Energy Consumption*

Power and energy meters (240V Wattnodes) with current transformers (CTs) were used to measure both the total heat pump system consumption (50A CTs) and indoor unit fan power (5A CTs). For ease of instrumentation, wiring was routed from the heat pump to a rated box mounted to the ceiling of the mechanical room (Figure 2.2).

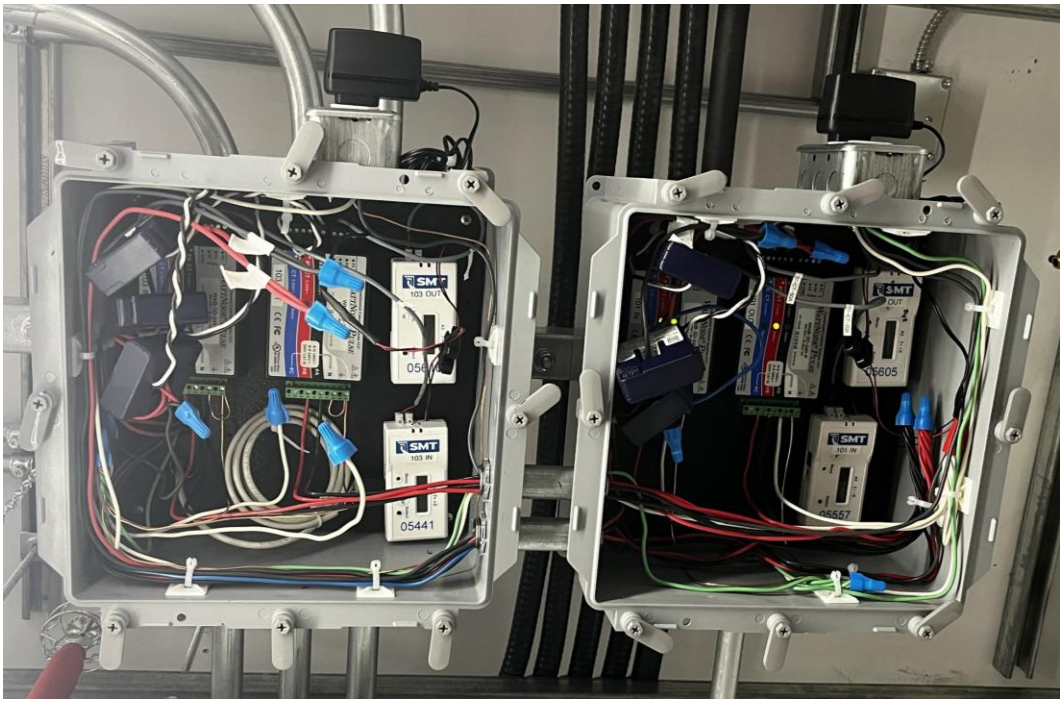


*Figure 2.2 – Ceiling mounted boxes in mechanical room for housing heat pump electricity consumption monitoring equipment.*

[3] Value from Mitsubishi Electric submittal data for MSZ-FS09NA-U1 & MUZ-FS09NAH-U1, 9000 BTU/H Wall-Mounted Cold Climate Heat Pump System, 2021.

## *Airflow Measurements*

To estimate the volumetric flow rate of air passing through the indoor units throughout the monitoring period, the volumetric flow rate was measured at each fan setting during the initial site visit. Indoor unit fans were sub-metered and used as a proxy for fan speed, to which measured flow rates were assigned depending on the fan speed setting. [4,5] The method used to determine the ductless mini split volumetric flow rate at the indoor unit supply was as follows (see Figure 2.3):

- → Secure an airtight box sealed around supply louver;
- → Connect the box to a variable speed fan;
- → Measure with a dual channel manometer:
  - → Pressure difference inside box in relation to the ambient indoor environment
  - → Pressure difference across the fan
- → Adjust fan speed until pressure difference is null between airtight box and indoor ambient environment (i.e. until CFM of variable speed fan matches CFM of the heat pump fan);
- → Record CFM across the variable speed fan;
- → Repeat for all heat pump fan speed settings.

*Figure 2.3 – Example of volumetric flow measurement apparatus mounted to a ductless mini split heat pump indoor unit.*

[4] Marleau, C. *BC Cold Climate Heat Pump Field Study*. Prepared for FortisBC, BC Hydro and the Ministry of Energy, Mines and Low Carbon Innovation. November, 2020.
[5] Williamson, J. and Robb, A. *Field Performance of Inverter-Drive Heat Pumps in Cold Climates*. Prepared for U.S. Department of Energy. August 2015.

## *Air Temperature and Relative Humidity*

Two air temperature (MF52 thermistor) sensors and one relative humidity (HTM2500) sensor were installed at each of the return and supply louvers of the heat pump indoor units (Units A & C, Figure 2.4). These parameters were monitored to determine the energy provided or removed by the heat pump. Outdoor ambient air temperature and relative humidity were also monitored on-site to correlate the efficiency of the units with outdoor conditions.

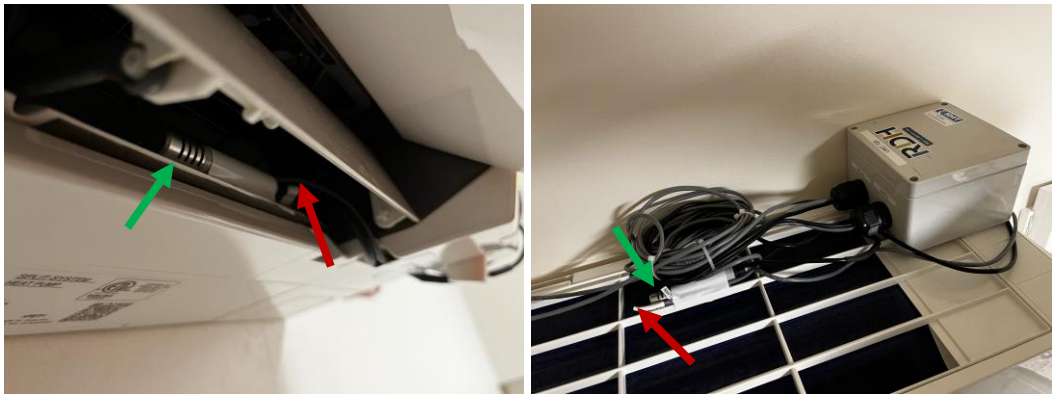

*Figure 2.4 – Example of temperature sensor (red arrow) and relative humidity sensor (green arrow) installation for an indoor unit at supply louver (bottom of unit, left image) and return grille (top of unit, right image).*

## *Hydronic Heating (Baseboard & Pre-Heating by HRV)*

Temperatures and flow rates of hot water for the hydronic baseboards and HRV were measured to estimate the heat delivered by the hydronic heating systems to the three units (Units A, B, and C). One temperature sensor (thermistor) was installed for the supply line, before branching off to supply individual units. Thermistors were installed on two return lines for units with heat pumps (Units A & C) and a return line for the control unit without a heat pump (Unit B). Thermistors were installed in contact with the pipes, under the pipe insulation. In-line flow meters were also installed at the return lines for all three units.

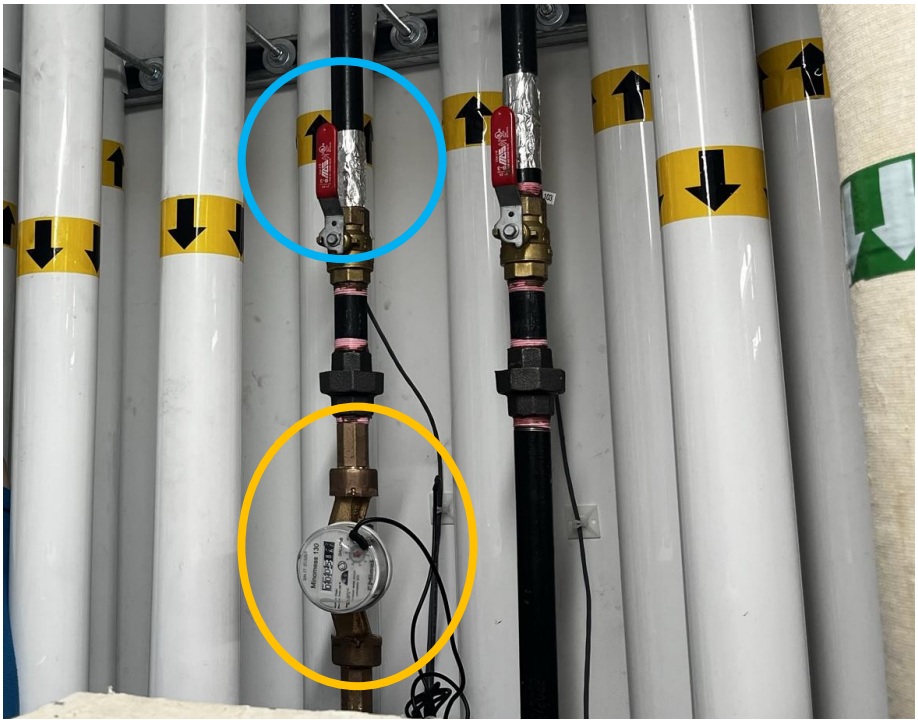

*Figure 2.5 – An example of in-line flow meter (yellow circle) installed on the return line for the hydronic heating system. Thermistors (blue circle) are taped upstream from the flowmeter with foil-faced tape. Note that pipe insulation was removed temporally to facilitate sensor install and was re-installed after the flow meter and thermistor were installed.*

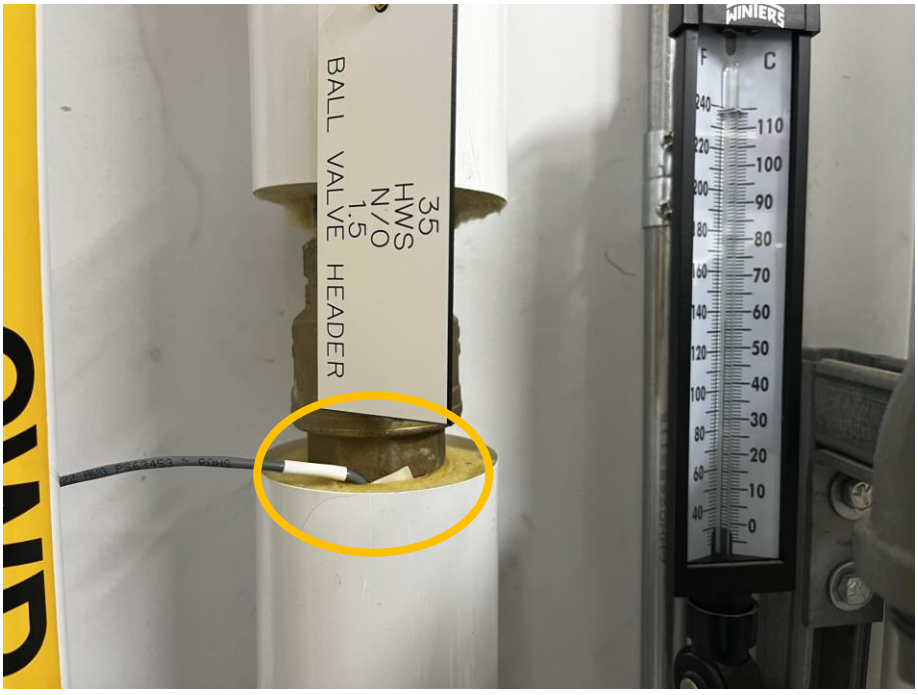


*Figure 2.6 – An example of completed thermistor installation after pipe insulation has been re-installed.*

## 2.3 Heat Pump Data Analysis

Data collected in the field are used to derive key heat pump performance metrics. This section describes the methodologies and assumptions used to conduct the analysis.

### *Energy Output*

Energy output of the heat pump system was determined using the following measurements:

- → Psychrometric properties of the supply and return air, derived from the measured dry-bulb temperatures and relative humidities;
- → Amount (mass) of air conditioned.

As discussed in Section 2.2, supply and return air temperatures and humidities were measured using thermistors and relative humidity sensors, respectively. The mass flow rate of the conditioned air was estimated using indoor fan energy consumption as a proxy, correlated to previously measured flow rates, rather than direct live measurements.

Because air source heat pump systems rely on convective heat transfer of forced air, the mass will typically enter the unit (return air grille) as a mixture of air and water vapour and match the mass of the exiting mixture (supply air louver). In a cooling process, however, water vapour can condense out of the supplied air when its dry-bulb temperature reaches its dew point temperature.[6] This cooling and dehumidification process is shown below in Figure 2.7.

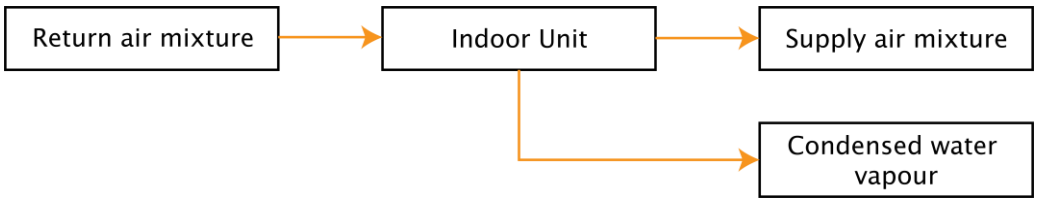


*Figure 2.7 – Mass flow through indoor unit under cooling and dehumidification.*

Latent energy generated by the phase change process of the return air from gas to liquid should, in theory increase the effectiveness of the cooling process since a greater amount of energy is being removed via a condensate drain before it is exhausted as supply air. Latent energy was included in heat pump performance when the difference in measured conditions between return and supply air suggest that condensation has occurred.[7]

For example, when the return air is cooled by the coil to a temperature below the air's dew point, less water vapour should be present in supply air. This process of cooling and dehumidification must satisfy a conservation of air mass and an energy balance between return and supply states.

[6] Dew point is the temperature at which the air becomes fully saturated and can no longer hold moisture in vapour form. In a cooling process, water vapour can condense out of supplied air when its dry-bulb temperature reaches the dew point - any further cooling beyond this point leads to condensation.
[7] ASHRAE (2017). Fundamentals (SI Edition).

The mass and energy balance equation for this case is described below:

$$\Delta E = \dot{V}_2 \rho_2 [(h_2 - h_1) - (W_2 - W_1) h_{w2}]$$

*Where subscript 1 refers to the return air, subscript 2 refers to the supply air, $\dot{V}$ is the volumetric flow rate (m³/s), $\rho$ is the density of the moist air mixture (kg/m³), $h$ is the specific enthalpy of moist air (kJ/kg), $W$ is the humidity ratio (kg/kg), and $h_w$ is the specific enthalpy of condensed water (kJ/kg).*

When measured conditions between return and supply air suggest that no condensation has occurred, the mass of the air entering the indoor unit (the return air) matches with the mass of the air exiting the indoor unit (the supply air), representing a sensible heating or cooling process. Note that a negative value will result when heat energy is removed, indicating a cooling process. The energy balance equation for this case is described below:

$$\Delta E = \dot{V}_2 \rho_2 (h_2 - h_1)$$

*Where subscript 1 refers to the return air, subscript 2 refers to the supply air, $\dot{V}$ is the volumetric flow rate (m³/s), $\rho$ is the density of the moist air mixture (kg/m³), and $h$ is the specific enthalpy of moist air (kJ/kg).*

## *Psychrometrics and Equipment Accuracy*

As described in the *Energy Output* section above, a mass and energy balance must be conserved through the conditioning process of the indoor unit. Therefore, in theory, it is possible to calculate an expected relative humidity of the supply air, based on the measured relative humidity of the return air. However, during an initial comparison between the measured and expected relative humidity, results suggested in some cases that the mass and energy balance were not conserved (i.e., expected did not match measured). This phenomenon is likely attributed to the accuracy of the instruments and affects the calculated performance of the studied heat pumps.

For the purposes of this study, it is important that the humidity ratio remains constant between supply and return air, particularly in heating mode when condensation would not take place. For example, an error in relative humidity measurement that would falsely suggest that moisture has been removed during the heating process could result in a significantly lower COP, as this would imply that some moisture-related energy was removed.

To identify the inherent error of the measurements made in this study, the following methods were used to preserve the mass and energy balance:

- → Calculate the measured partial vapour pressure of the return and supply states of air using the measured dry-bulb temperature and relative humidity
- → Calculate the expected partial vapour pressure of the supply state of air by equating it to the measured specific vapour pressure of the return state.
- → Calculate the expected relative humidity of the supply state of air knowing the expected partial vapour pressure.
- → Check the agreement between the expected and measured relative humidity of the supply state of air.

The methodology used to evaluate agreement between the expected and measured values of relative humidity was to compare the range of uncertainty via the combination of errors

in quadrature, also known as the square root of the sum of squares.[8] Listed accuracy for the instruments allowed the computation of uncertainty ranges for each measurement and their calculated derivatives. The agreement between the expected and measured values was evaluated based on the propagated error of both calculated values and is related to the accuracy of the instruments used. This process is illustrated in Figure 2.8. This technique reduced the variability of the calculated heat pump performance from the overall sample of collected data.

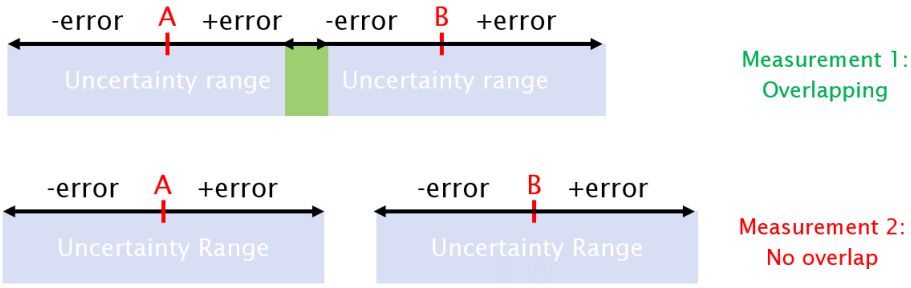


*Figure 2.8 – examples of propagated error between two calculated values. In this example, Measurement 1 would be accepted as its error band (B) overlaps with expected result's error band (A). Measurement 2 error band (B) does not overlap with expected error band (A) and therefore would be rejected.*

## *Assumptions for Filtering Logic and COP Calculations*

The criteria to determine whether the heat pump is actively heating and cooling (and therefore to determine what periods are included in the COP calculations) are outlined in Table 2.1 below.

TABLE 2.1 HEATING AND COOLING CRITERIA (5-MINUTE DATA)

| **Parameters** | **Heating** | **Cooling** |
|---|---|---|
| Difference in supply and return temperatures ($T_{supply}$-$T_{return}$); and | ≥ 5˚C | ≤ -5˚C |
| Indoor fan operation (5A CT); and | > 0 pulse | |
| System consumption (50A CT) | > 0.01 kWh | |

The system consumption threshold was selected to be above typical electricity consumption (over a five-minute period) during fan-only mode in the summer. As the supply and return temperatures of the heat pump system were measured in close proximity, the effects of hydronic baseboard operation on these temperatures were assumed to be similar. Thus, heat pump system output, derived from the difference in supply and return temperatures and relative humidities, was calculated independent of hydronic baseboard operation.

The criteria to identify the start and the end of a defrost cycle is outlined in Table 2.2.

[8] Wolfram (2019) Experimental Data Analyst Documentation. Available online: https://reference.wolfram.com/applications/eda/ExperimentalErrorsAndErrorAnalysis.html

| TABLE 2.2 DEFROST CRITERIA (5-MINUTE DATA) | | |
|---|---|---|
| **Parameters** | | **Defrost** |
| Start | Supply temperature ($T_{supply}$); and | Change ≤ -7˚C |
| | System consumption (50A CT); and | ≥ 0.03 kWh |
| | Outdoor air temperature | ≤ 10˚C |
| End | Supply temperature ($T_{supply}$); and | ≥ $T_{supply}$ at start |
| | System consumption (50A CT) | Local maximum |
| | Or, Defrost cycle length | ≥ 30 minutes |

Local peak consumption (more than the five-minute periods before and after) is used to identify the end of the defrost cycle because consumption was observed to spike at the end of the defrost cycle, when the compressor operates continuously to raise the supply temperature back to the typical heating range. Otherwise, defrost cycles were assumed to continue for a maximum length of 30 minutes.

Based on the definitions outlined above, periods of heating/cooling and defrost were identified. While simultaneous heating and defrost is not theoretically possible due to the direction of the refrigeration cycles being opposite, the indoor fan is not always off during defrost, and supply temperature of the heat pump sometimes remain at least 5˚C higher than the return temperature from residual heat. As a result, the heat pump system is supplying heat to the indoor environment based on the heating criteria above.

## 2.4 Hydronic Heating Data Analysis

For the units in which both the heat pump and hydronic heating system are used, the two are connected via a smart thermostat to control how and when each system is used during the heating season. In this study, the heating energy delivered by the baseboards and for pre-heating with the in-suite heat recovery ventilator (HRV) are grouped together. The intended controls strategy is for the heat pump to serve as the primary heating system when the outdoor air temperature is at or above -30˚C, while the hydronic baseboard is supplemental and comes on when the outdoor air temperature is below the threshold, or when the heat pump alone cannot meet the interior set point.

To understand the overall performance of this system, the heating energy supplied by the hydronic system needs to be calculated. 100% of the energy supplied by the hydronic system is assumed to be delivered to the room either via baseboards, HRV, or losses through pipe insulation. The amount of heat being supplied by the hydronic system can be estimated from the temperature difference between the supply and return hydronic piping, as well as the volume of water that flows through the water loop. The energy output by hydronic system is described below:

$$\Delta E = \dot{V} \cdot \rho \cdot C_p \cdot (\mathrm{T}_2 - \mathrm{T}_1)$$

*Where $\dot{V}$ is the volumetric flow rate through the hydronic piping, $\rho$ is the density of water, $C_p$ is the specific heat capacity of water, $T_1$ is the temperature in the return hydronic piping, and $T_2$ is the temperature in the supply hydronic piping.*[9]

The energy delivered during the five-minute interval was assumed to be zero if either of the supply or return temperatures were reported to be outside the theoretical range of 0˚C to 100˚C, or if an error returned for the flow rate measurement. These periods account for less than 1% of the available data.

[9] ASHRAE (2017). Fundamentals (SI Edition)

# 3 Results & Discussion

As described above, a total of three units in the 8-plex were monitored. Table 3.1 summarizes the naming conventions for the units and the corresponding heating systems that were measured.

TABLE 3.1 NOMENCLATURE AND CORRESPONDING MEASURED HEATING SYSTEMS

| Location | Heating Systems |
|---|---|
| Unit A | heat pump, hydronic baseboards, HRV |
| Unit B (control) | hydronic baseboards, HRV |
| Unit C | heat pump, hydronic baseboards, HRV |

## 3.1 Non-Routine Adjustments

Adjustments were made to the heating system controls and the monitoring equipment over the course of the study:

- 20A CTs were swapped to 5A CTs to monitor indoor fan operation in April 2023 to improve data resolution.
- Irregularities in the data became apparent after installing 5A CTs to improve resolution. An incorrect AC adaptor was identified as the cause, affecting readings from the outdoor temperature and RH sensors, as well as energy measurements from the 50A CTs (heat pump total energy consumption) and 5A CTs (fan energy consumption). The adaptor was replaced with the correct 4.5V model on April 20, 2023; however, data collected prior to this correction is considered unreliable.
- Controls in Unit A were updated several times; in early 2023, at the end of April 2023, and then again in early May 2023.

## 3.2 Heat Pump Performance

### 3.2.1 Volumetric Airflow Rate

As described in Section 2.2, the volumetric airflow rate of a heat pump indoor unit was measured at all fan settings and compared with manufacturer data sheets. Figure 3.1 shows the measured and estimated volumetric flow rates compared to manufacturer data.

Results show that the measured volumetric flow rates in cooling mode were slightly less (about 94%) compared to rated values. Note that during the initial site visit, the ambient outdoor temperature was below -30˚C and therefore airflow rates could not be measured in heating mode. Therefore, the heating mode airflow rate was estimated based on the measured airflow rate in cooling mode.

In interpreting the discrepancy between the measured/estimated airflow rates (via the plenum method described in Figure 2.3) and the manufacturer's rated volumetric flow, the measurement methodology itself is unlikely to have introduced a significant bias. The plenum used during testing was larger than the indoor unit discharge and was pressure-balanced to the surrounding indoor environment ($\Delta P \approx 0$ Pa). Under these conditions, the

fan of the variable-speed reference blower effectively matched the mini split fan output without creating additional airflow restriction or introducing higher pressures at the supply.

The lower field-measured airflow rates relative to manufacturer ratings have previously been observed and documented in NREL studies: *Field Validation of Air-Source Heat Pumps for Cold Climates*[10] and *Field Performance of Inverter-Driven Heat Pumps in Cold Climates*,[11] and are likely due to field conditions rather than measurement bias. Manufacturer ratings are established under idealized laboratory conditions with minimal external resistance, whereas field installations include return filters, coil resistance, and variations in air density and test environment. The position of adjustable louvers is also confirmed as a factor that dramatically affects airflow rates.[11]

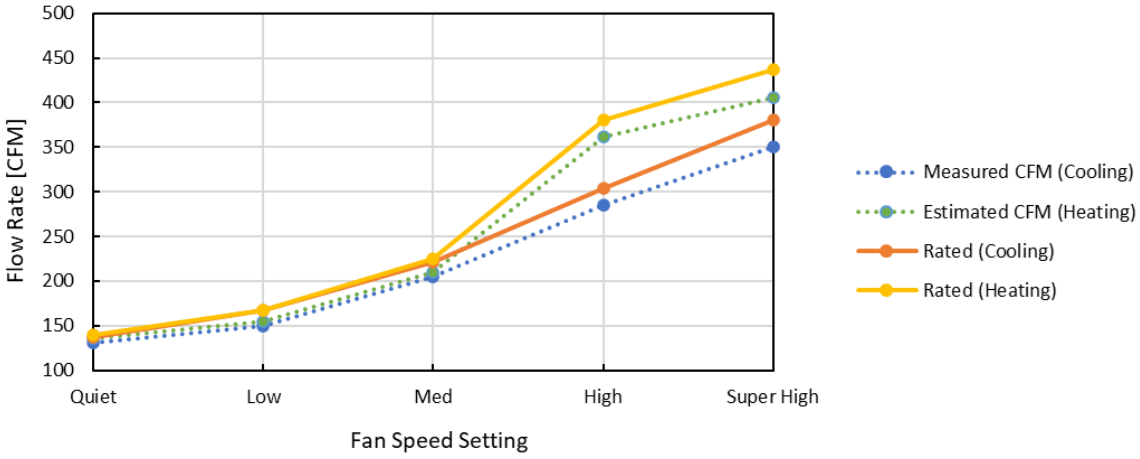


*Figure 3.1 – Measured and estimated volumetric flow rates compared to manufacturer data.*

### 3.2.2 Monitoring Results (May 1, 2023 to December 31, 2024)

This section describes results for the monitoring period between May 1, 2023 and December 31, 2024 (the entire period for which we have reliable data).

Figure 3.2 shows the number of data points collected during heat pump heating or cooling operation in Units A and C over this period.

[10] NREL/TP-5500-84745 (2023) – Field Validation of Air-Source Heat Pumps for Cold Climates, National Renewable Energy Laboratory. https://www.nrel.gov/docs/fy23osti/84745.pdf
[11] NREL/TP-5500-63913 (2015) – Field Performance of Inverter-Driven Heat Pumps in Cold Climates, National Renewable Energy Laboratory. https://www.nrel.gov/docs/fy15osti/63913.pdf

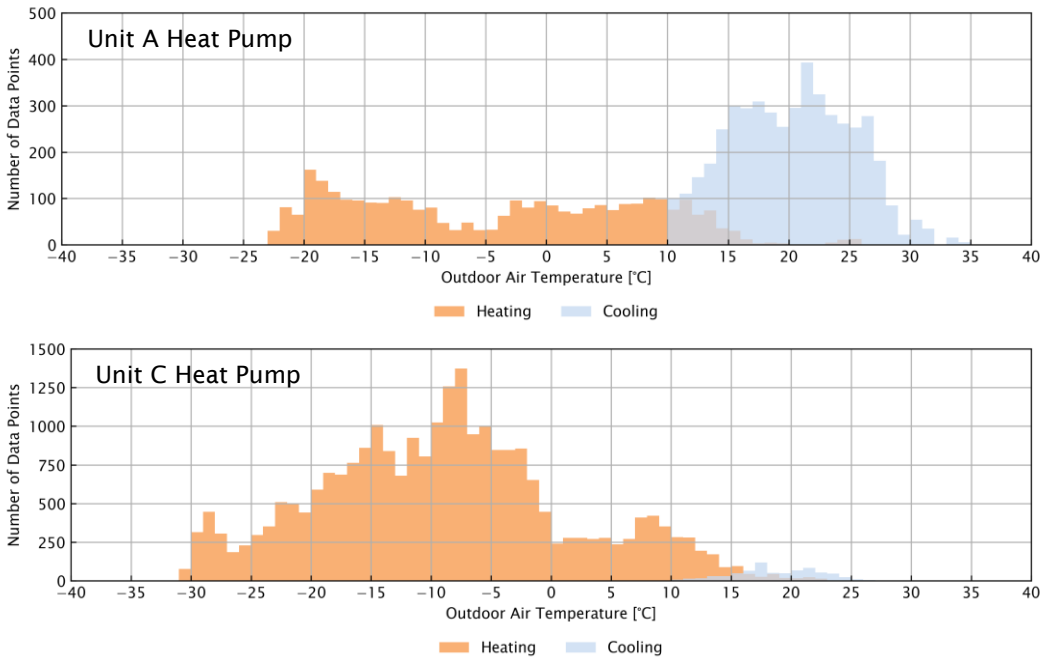


*Figure 3.2 – Number of data points (5-min intervals) for the heat pumps in Unit A (above) and Unit C (below) for the period between May 1, 2023 and December 31, 2024. Note the different y-axis ranges.*

This figure indicates that more data points were obtained for Unit C than for Unit A over the two-year monitoring period. Reasons for this include the following:

- In Unit A, for a period from October 30, 2023 to the beginning of January 5, 2024, there was a break in data collection due to two consecutive battery failures (with a small period on December 4, 2023 where the first replacement was operational). There was another battery failure in October 2024 which was replaced on November 14, 2024.
- Control issues were observed between the heat pump and baseboards in Unit A (this will be further discussed in later sections). In short, the heat pump is intended to be the primary heating source when outdoor ambient temperatures are above -30˚C. However, it appears that even after the modifications to the controls (around the end of April 2023 and beginning of May 2023), the hydronic heating was operating far more often than the heat pump, even when outdoor temperatures are above -30˚C. A more detailed analysis of hydronic heating is provided in Section 3.3.
- Note, that while Unit C has a lot more data points overall, most of these are in heating mode. In fact, Unit A has more data points in cooling mode than Unit C.

Figure 3.3 and Figure 3.4 display the measured ambient outdoor temperature, the temperatures at indoor unit supply/return, and the equivalent energy provided or removed by heat pump compared to total energy consumption for Units A and C, respectively.

The graphs demonstrate a few key findings:

- For both Units A and C, during the summer 2023 and 2024 periods, the heat pumps were off most of the time (i.e. there is a significantly lower energy consumption for heating than other times in the year and very little cooling energy consumption), as outdoor temperatures hover around 20°C.
- As expected, the heat pumps are turned off when outdoor ambient temperatures are below -30˚C, allowing for heating from hydronic baseboards to take over during the colder periods. One example is at the start of January 2024. This is particularly obvious in the heat pump energy consumption plot for Unit C (Figure 3.4). We see that when the outdoor temperature drops below -30˚C at the beginning of January, the heat pump turns off, and stays off until outdoor temperature increases above -30˚C.
- Notable differences between Units A and C emerge in winter 2023/2024. Unit C (Figure 3.4) frequently records energy supplied/removed to the space exceeding 0.15 kWh in five minutes, whereas for Unit A (Figure 3.3), such values are rare exceptions, despite both units having similar levels of system energy consumption. Notably, the heat pump in Unit C demonstrates significantly better performance (i.e. higher coefficient of performance) compared to Unit A. This same pattern persists into winter 2024/2025.
- Unique or anomalous readings (e.g., data loss for Unit A) are annotated for further clarification.

Unit A Heat Pump

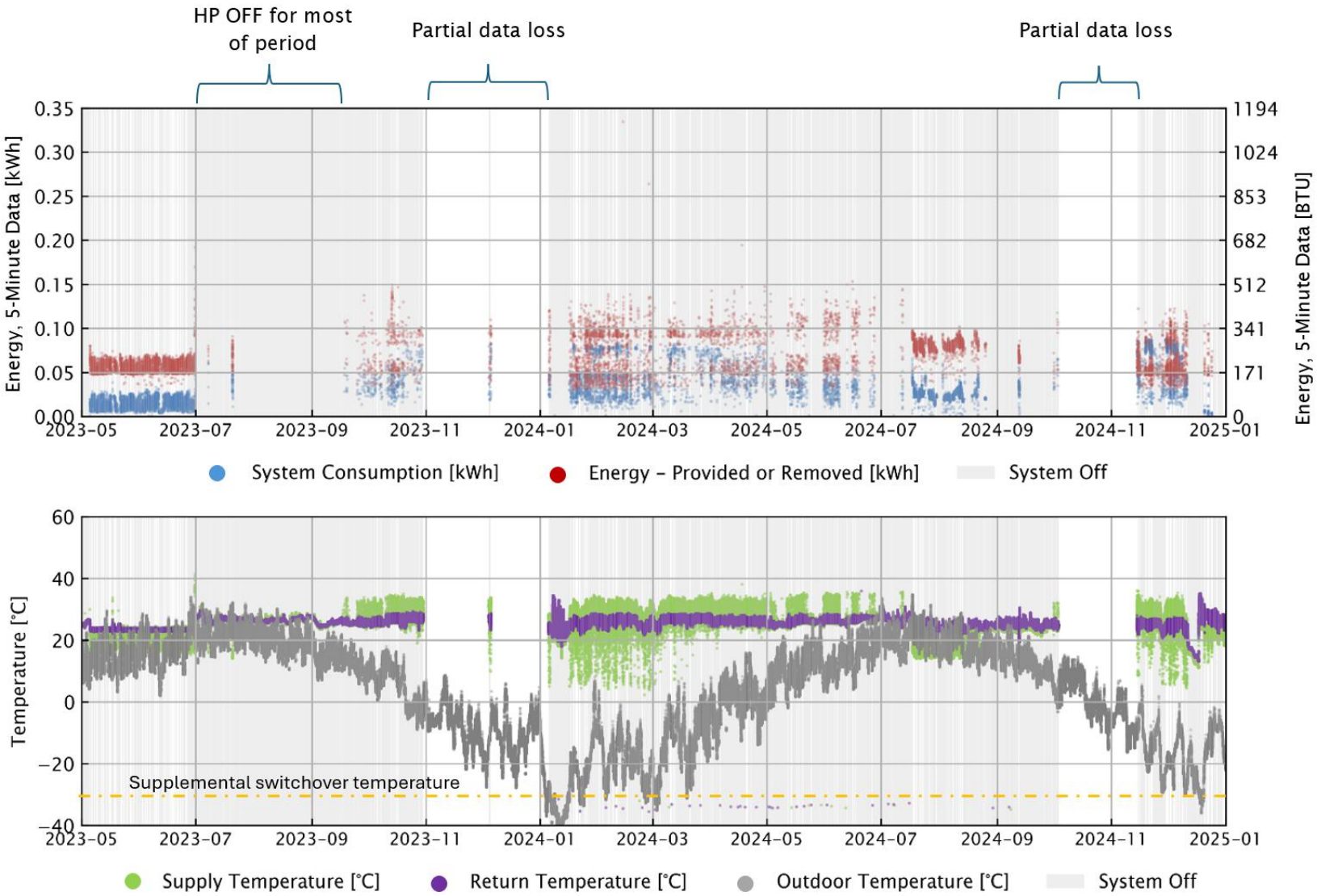


*Figure 3.3 – Measured ambient outdoor temperature and temperatures at indoor unit supply/return (bottom), and equivalent energy provided/removed by heat pump compared to total energy consumption (top) for Unit A.*

Unit C Heat Pump

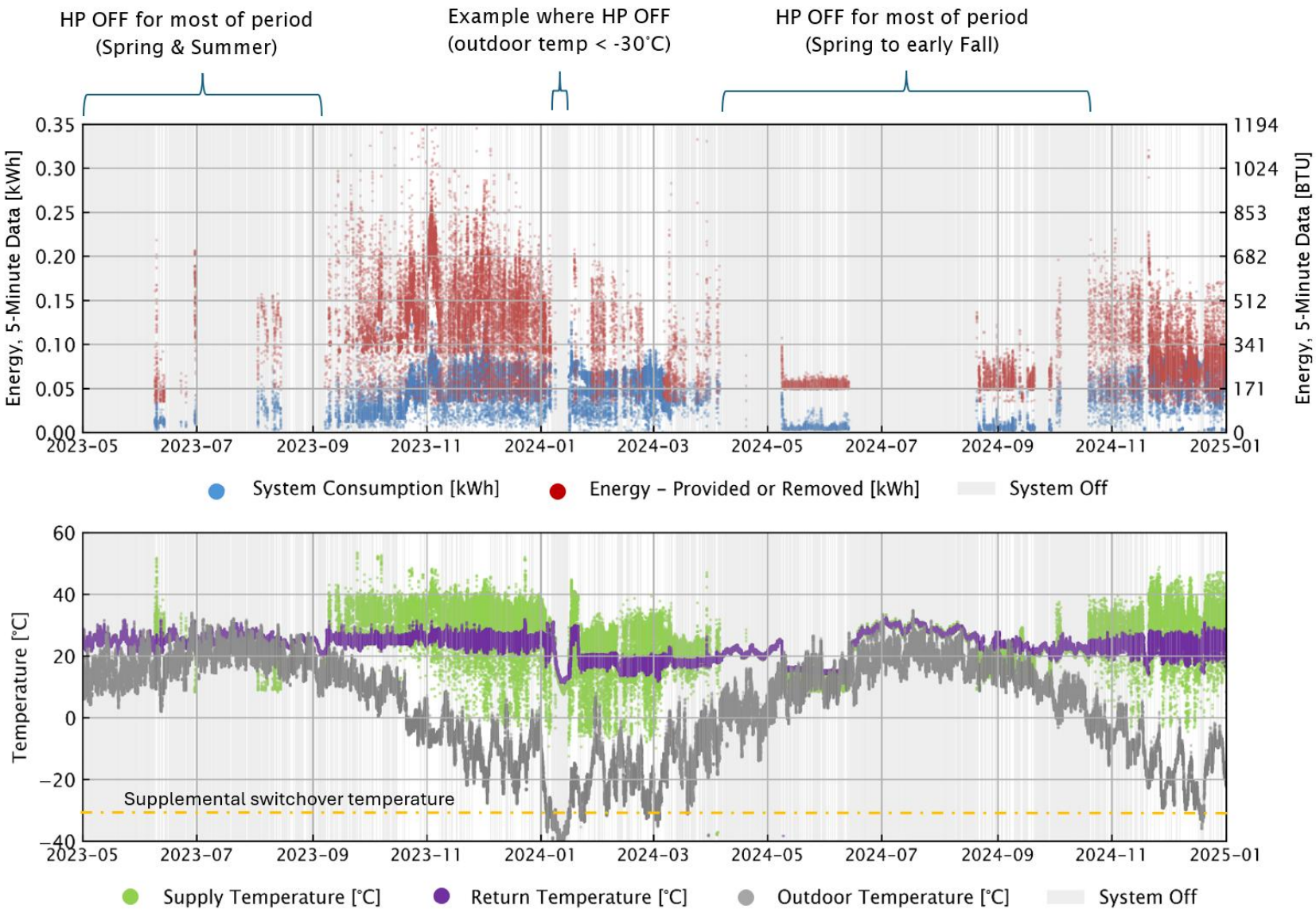


*Figure 3.4 – Measured ambient outdoor temperature and temperatures at indoor unit supply/return (bottom), and equivalent energy provided/removed by heat pump compared to energy consumption (top) for Unit C.*

## *Coefficient of Performance*

The coefficient of performance (COP) is a common metric for measuring the efficiency of heat pumps. It can be defined as a ratio of energy delivered to or removed from a space relative to the energy required by the system to perform the work. A COP greater than 1 indicates that the energy provided or removed is greater than the energy consumed by the heat pump. Heating and cooling seasonal COPs (SCOPs) are presented in Table 3.2 and Table 3.3 below, respectively. Each SCOP value is presented alongside the "average outdoor temperature during operation," calculated based on the subset of data points where the heat pump was actively operating in the relevant mode ('heating' or 'cooling') and for which the SCOP was determined.

TABLE 3.2 HEATING SEASONAL COP

| Data Period | Unit A | | | Unit C | | |
|---|---|---|---|---|---|---|
| | Number of Data Points, N | Average Outdoor Temperature During Operation [°C] | Measured SCOP | Number of Data Points, N | Average Outdoor Temperature During Operation [°C] | Measured SCOP |
| May 1 to June 30, 2023 | 33 | 24.3 | 4.3 | 267 | 14.5 | 4.4 |
| July 1, 2023 to June 30, 2024 | 2021 | 1.5 | 1.7 | 16854 | -5.5 | 2.7 |
| July 1 to December 31, 2024 | 1065 | -14.1 | 0.8 | 7980 | -15.4 | 1.4 |

Notes:

This table considers data points during "Heating," or "Defrost" when the system is not "Cooling", based on the criteria described in Section 2.3.

Heating seasonal COP (SCOP) is the sum of heating output divided by the sum of energy consumption for the subset of data points.

The corresponding number of data points (N) and the average outdoor temperature are also reported.

The SCOP for Unit A for the May 1 to June 30, 2023 period has been presented in this table; however, with only 33 data points, it is not deemed statistically significant.

| TABLE 3.3 COOLING SEASONAL COP | | | | | | |
|---|---|---|---|---|---|---|
| Data Period | Unit A | | | Unit C | | |
| | Number of Data Points, N | Average Outdoor Temperature During Operation [˚C] | Measured SCOP | Number of Data Points, N | Average Outdoor Temperature During Operation [˚C] | Measured SCOP |
| May 1 to December 31, 2023 | 2727 | 18.5 | 3.6 | 284 | 22.1 | 4.9 |
| January 1 to December 31, 2024 | 2015 | 23.7 | 3.2 | 446 | 17.5 | 4.1 |

Notes:

This table considers data points during "Cooling," based on the criteria described in Section 2.3.

Cooling seasonal COP (SCOP) is the average COP for the subset of data points.

The corresponding number of data points (N) and the average outdoor temperature are also reported.

Figure 3.5 is a plot of the average heating and cooling COPs for Units A and C at various outdoor operating conditions determined using the data from May 1, 2023 through December 31, 2024.

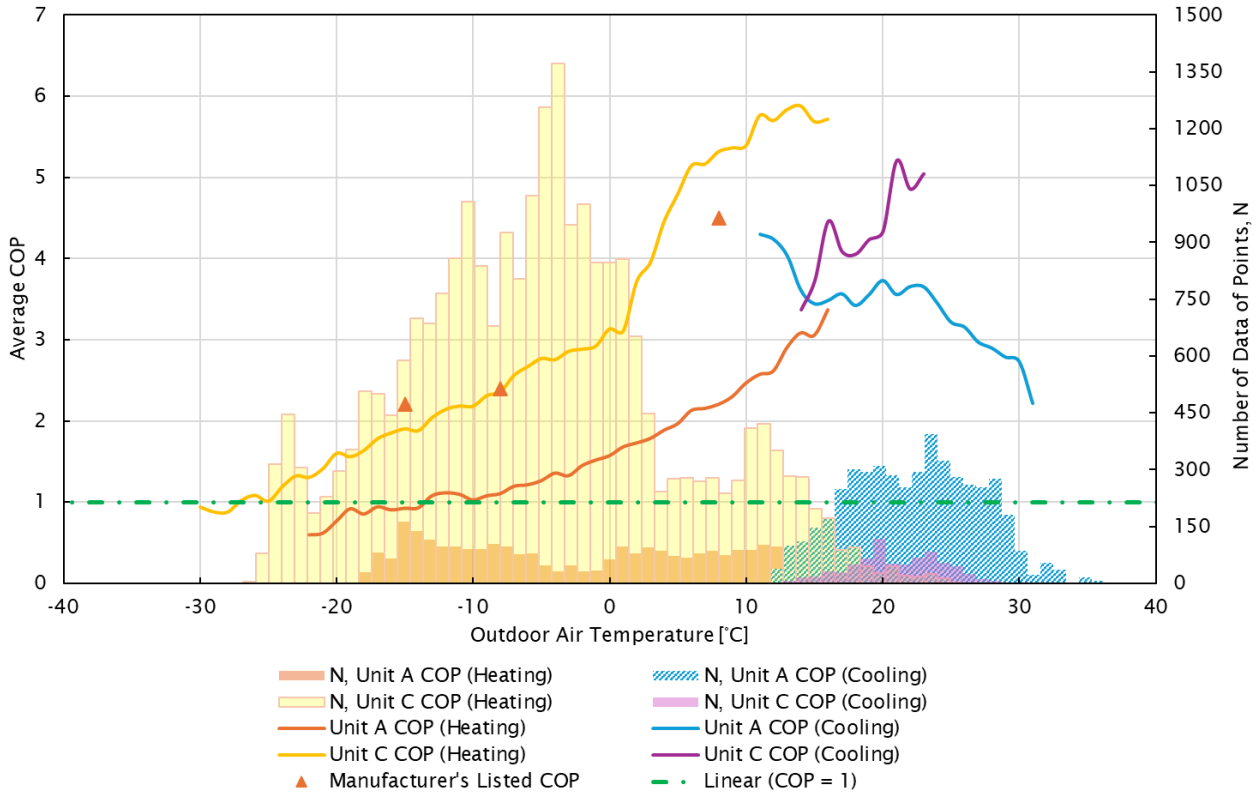


*Figure 3.5 – Heat pump average heating and cooling COPs at various outdoor operating conditions for the monitoring period between May 1, 2023 and Dec. 31, 2024 are plotted as various line plots on the primary y-axis. The number of data points collected during this period, N, are plotted on the secondary y-axis.*

The data in Figure 3.5 show the following:

1. It appears that Unit C's heat pump has a higher COP than Unit A, and that the Unit C heat pump closely follows the manufacturer's listed COP values. As briefly discussed in the previous interim reports, the control strategy for Unit A's heat pump and hydronic heating was not configured properly initially, and they were operating simultaneously causing the heat pump to short cycle. Although this problem was purported to be solved in May 2023, we suspect that the control problems continued through to the end of the project and is affecting the heat pump in Unit A's performance. In contrast, Unit C's control strategy (i.e., heat pump as the primary heating source when outdoor ambient conditions are above -30˚C) allowed for the heat pump to operate without notable interference from the hydronic heating system. This allowed for longer heating cycles and overall better COP. The missing data from Unit A over the fall/winter months for portions of 2023 and 2024 are also anticipated to be impacting the results for Unit A COP.
2. In cooling mode, both units exhibit average cooling COPs above 2. However, the data from Units A and C do not show strong agreement. Unit A operated in cooling mode significantly more frequently than Unit C, as illustrated by the number of data points shown on the secondary y-axis of Figure 3.5. For Unit A, a clear trend is observed: the average cooling COP decreases with increasing outdoor air temperature, which aligns with expected thermodynamic behavior. Specifically, the average cooling COP declines from approximately 4.3 at 11˚C to about 2.7 at 30˚C. In contrast, Unit C has limited data in cooling mode, preventing a well-defined correlation with outdoor temperature. Reasons for this could be because the tenant in Unit C relies more on passive cooling (e.g., opening windows), simply does not use the system for cooling, or if the unit were unoccupied for a period. Nonetheless, its average cooling COP fluctuates between 3.3 and 5.0 over the temperature range of approximately 14˚C to 23˚C.
3. The distinct upward bend of the heating COP line for Unit C in Figure 3.5 near 1˚C likely reflects a rapid improvement in compressor efficiency as the outdoor temperature rises through the freezing range. Around this point, the refrigerant's evaporating pressure increases sharply while the condensing pressure remains relatively stable, causing the compressor pressure ratio and the required compression work to drop quickly. This creates a short interval where small increases in outdoor temperature produce disproportionately large gains in COP. As the outdoor temperature continues to rise beyond approximately 5 ˚C, the evaporating pressure stabilizes and the compression ratio changes more gradually, resulting in a smoother, near linear COP trend. This behavior is consistent with the thermodynamic relationship between compression ratio and heat pump efficiency described by Yu et al. (2023)[12] and Frik et al. (2024)[13].

Another way to visualize the efficiency of the heat pumps and provide further context is to plot the average power output to the space (for both heating and cooling), and the corresponding power consumption at the various outdoor operating conditions (Figure 3.6). Theoretically, when the power output dips below the power consumption, the units are operating at a COP that is less than 1. In previous reports for this project, we found that output and consumption lines did not intersect at low outdoor temperatures as would

[12] Yu Z. et al. (2023). *A unified approach for the thermodynamic comparison of heat-pump cycles. Commun Eng 2, 62. Climate and Atmospheric Science*, 6(1). https://www.nature.com/articles/s44172-023-00112-0

[13] Frik A. et al. (2024). *Experimental Studies and Performance Characteristics of Air-Source Heat Pumps at Low Ambient Temperatures. Applied Sciences,* 14(9): 3933. https://www.mdpi.com/2076-3417/14/9/3933

be expected because of limited data. However, for this figure we see that for Unit A this intersection occurs at approximately -14°C, and for Unit C this intersection occurs at -26°C or -27°C. This agrees with the temperatures at which we saw the heat pumps have an average heating COP of 1 in Figure 3.5.

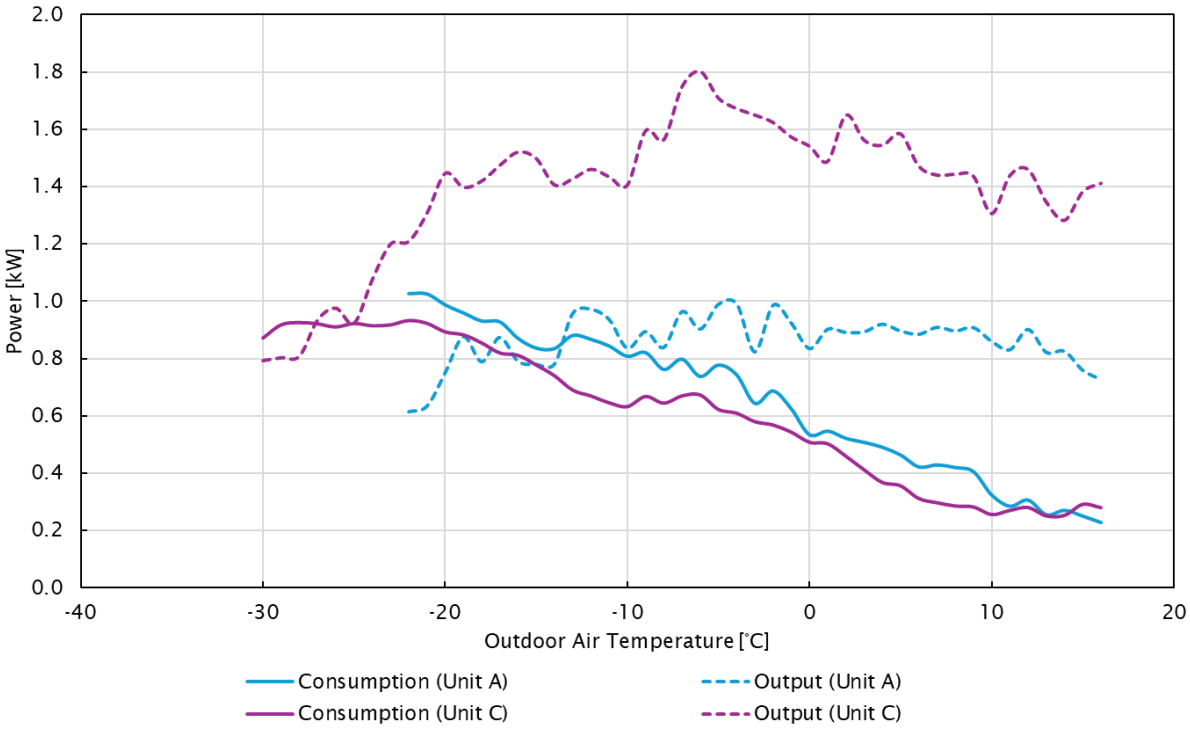


*Figure 3.6 – Heat pump consumption and output (for heating and cooling) at various outdoor operating conditions for the monitoring period from May 1, 2023 to December 31, 2024.*

As shown in Figure 3.7, during RDH's site visit in November 2024, the mini split indoor unit filter in Unit A was found to be completely clogged. A clogged filter can significantly impair system efficiency by restricting airflow, which may have impacted the unit's performance. If the filter had been obstructed for an extended period, this could partially account for the observed performance differences between Unit A and Unit C. In contrast, Unit C was found to be operating without a filter at the time of the visit, though it remains unclear when the filter was removed. We can therefore attribute the relatively poorer performance of the heat pump in Unit A to control issues, lack of synergy with the hydronic heating system, and the clogged filter.

*Figure 3.7 – Dirty filter from Unit A (left) and missing filter in Unit C (right) as observed in November 2024.*

Figure 3.8 shows sample daily plots of heat pump operation for Units A and C on January 29, 2024. The top figure illustrates how the heat pump in Unit A is operating simultaneously with the hydronic heating between midnight and 10am. However, since the outdoor ambient air temperature remains above -30˚C, hydronic heating is not expected to be operating for long extents of time. Unit C's operation (bottom figure) is more representative of expected behaviour, with the hydronic system remaining off, as would be expected in these temperature conditions.

Another observation is that the supply temperature regularly dips below the return temperatures during periods of low outdoor air temperatures (below approximately -10˚C). This indicates defrost cycles, when the heat pump temporarily reverses to send heat to the outdoor unit instead of the interior space.

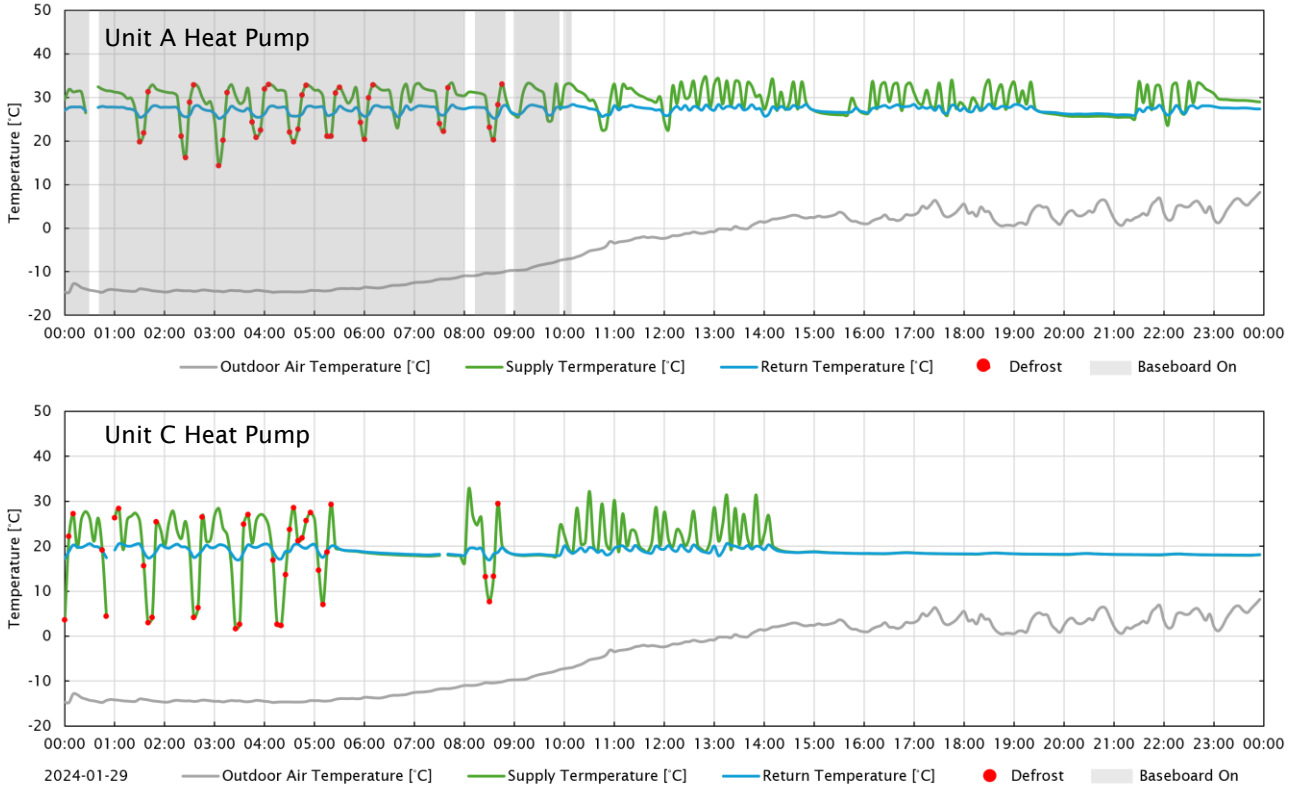


*Figure 3.8 – Heat pump cycles for Unit A (top) and Unit C (bottom) during a sample day on January 29, 2024. The blue and green lines show the return and supply temperatures of the heat pump, respectively.*

In summary, the data suggest that the heat pump systems can maintain a COP greater than 1.0 down to roughly -26˚C/-27˚C. This is particularly evident based on the heat pump in Unit C, which appears to be operating optimally.

As discussed previously, the issues with the non-optimized controls between Unit A's heat pump and hydronic heating has shown to negatively affect the performance of the heat pump.

### *Heating Demand and Capacity*

The measured heating capacity of the heat pumps was compared to the modeled heating demand, based on EnerGuide Home Evaluation reports for Units A and C.

Figure 3.9 shows the maximum and minimum capacities of the heat pump units based on the manufacturer's equipment submittal (dashed lines) for the entire monitoring period for the study. The modeled heating demand of Units A and C are shown in orange and yellow, respectively. The blue and green dots represent the average measured heating capacity of the heat pumps in Units A and C, respectively. Based on these averages, the balance point temperature (i.e. when capacity and demand intersect) is around -10˚C to -20˚C. In theory, to maintain thermal comfort, the intersecting point should be at -30˚C, as the heat pumps are supposed to be providing enough heat to the spaces down to that setpoint. However, the maximum heating energy provided, at least for Unit C (solid green line) is both tracking the manufacturer's maximum capacity and is converging with the heating demand around -26˚C.

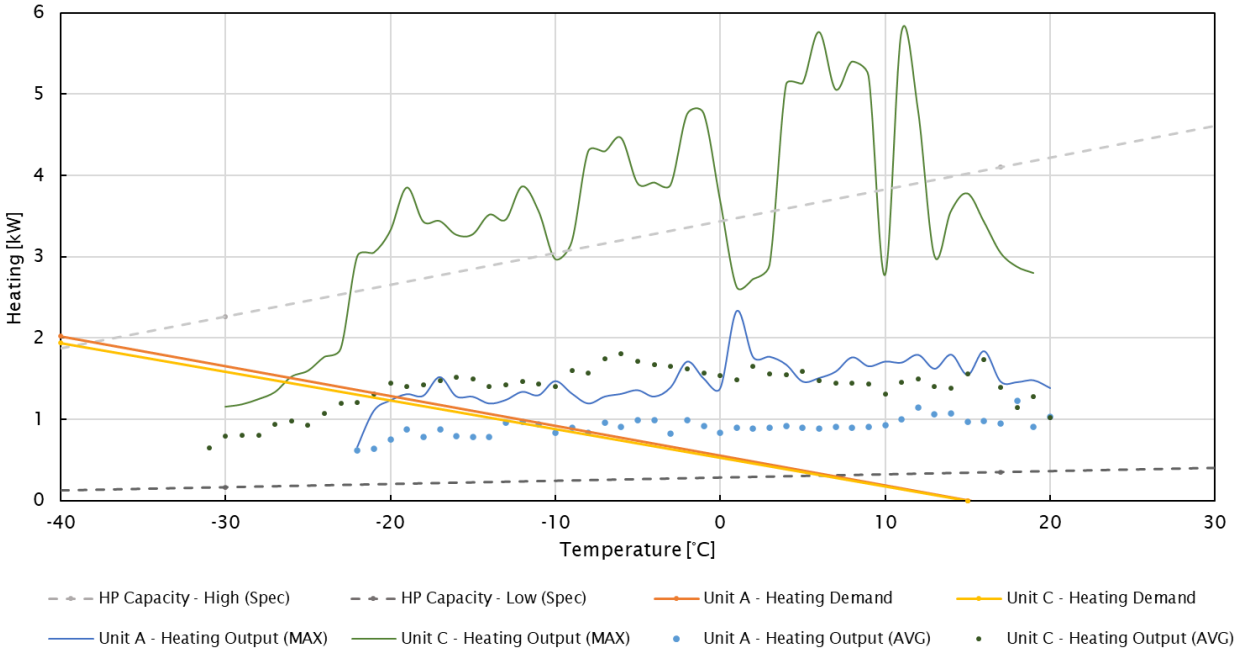


*Figure 3.9 – Measured heating output (average & maximum) compared to modeled heating demand (EnerGuide) for the monitoring period from May 1, 2023 to December 31, 2024.*

## 3.3 Hydronic Heating

This section presents general observations and findings from the monitoring of the hydronic heating systems (baseboard and pre-heating with HRV). As mentioned in Section 2.1, heat pumps were intended to serve as the primary heating system in Units A and C, with hydronic heating turning on only when the outdoor temperature is below -30˚C or when the heat pump alone cannot meet the interior set point.

Figure 3.10 is a timeseries plot of the daily energy delivered from hydronic heating from the monitoring period between May 1, 2023 and December 31, 2024.

Unit C's behaviour closely follows what is expected if the controls strategy was properly implemented. We see that the hydronic system turns on when the outdoor temperatures fall below -30˚C.

Looking at Unit A, consistent with findings in Section 3.2.2, it appears that Unit A hydronic system operates when the outdoor temperature was at or above the -30°C threshold (even after controls were purported to be adjusted). This indicates that the controls strategy may still be less than optimal. Note that outdoor air temperature shown in Figure 3.10 is the daily average (not minimum). In many instances, the daily energy delivered in Unit A was also greater than in the control unit (Unit B).

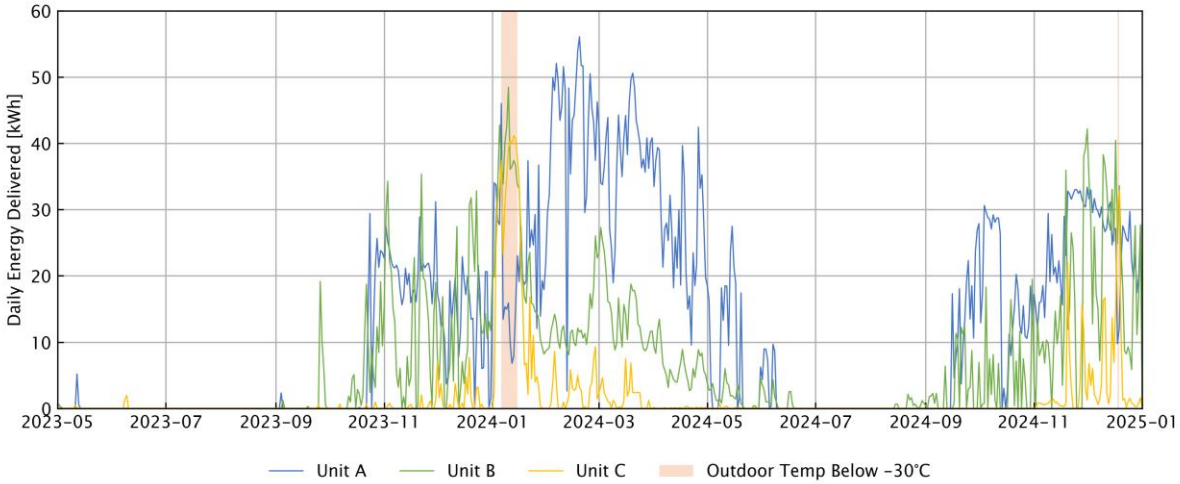


*Figure 3.10 – Daily total hydronic heating energy delivered for Units A, B, and C. Outdoor air temperature used for determining periods below -30˚C in this graph is the daily average.*

Figure 3.11 presents the monthly heating energy delivered by the hydronic heating system for the May 1, 2023 to December 1, 2024 reporting period. Comparing the three units during the spring months, Unit B (control; hydronic heating only) had higher hydronic usage than Unit C, but did not consistently have higher usage than Unit A. The higher usage by Unit A for most months is most likely attributed to the aforementioned control issue.

In general, the usage of hydronic system as supplemental heating decreases as outdoor temperature increases. However, the outdoor temperature at which residents turn off the hydronic heating varies between the units due to differing preferences.

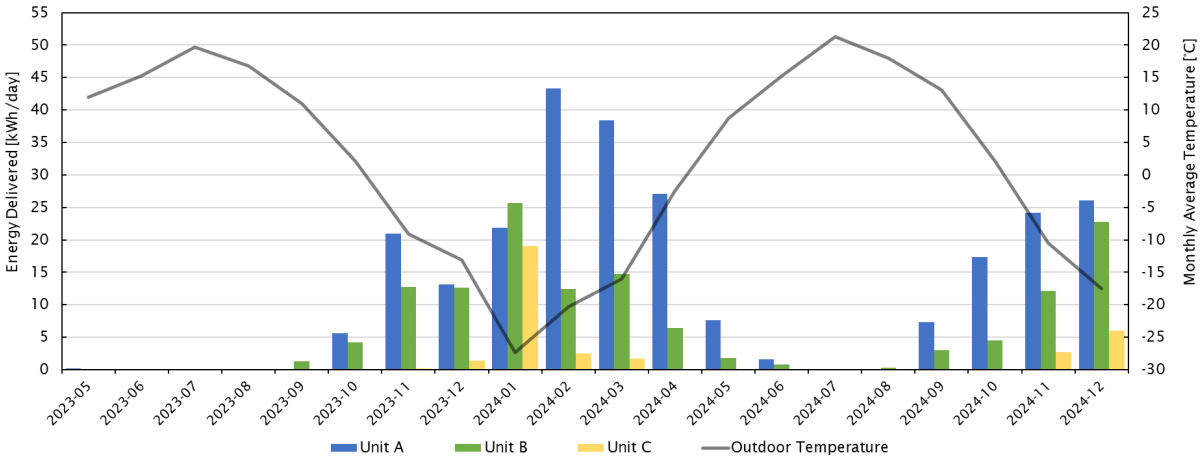


*Figure 3.11 – Monthly total hydronic heating energy delivered, normalized by the number of days in each month.*

For comparison, Figure 3.12 below is a plot of the monthly energy delivered by the heat pumps.

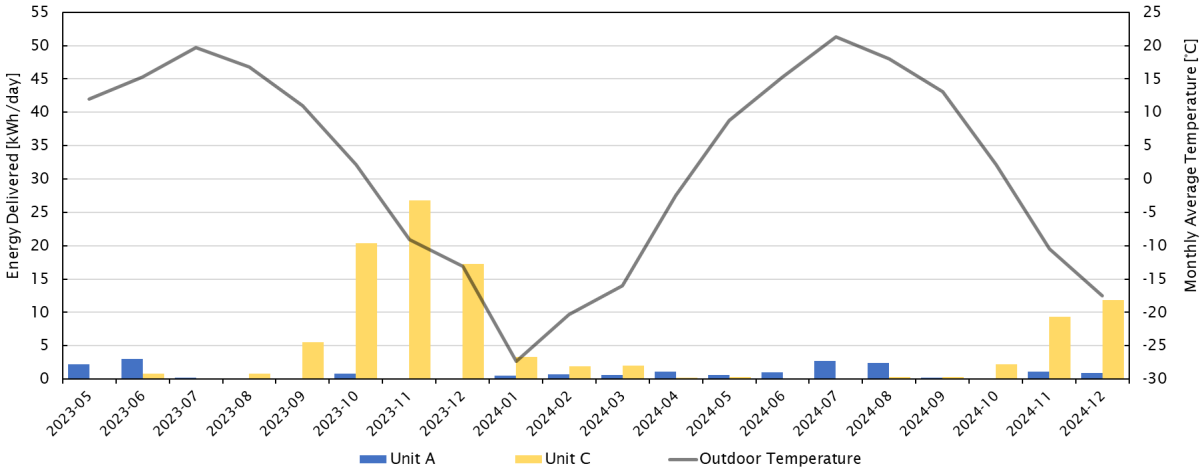


*Figure 3.12 – Monthly total heat pump energy delivered, normalized by the number of days in each month.*

Figure 3.13 presents the above data in a slightly different way and shows the percent of home heating provided by the heat pump versus hydronic heating for Units A and C.

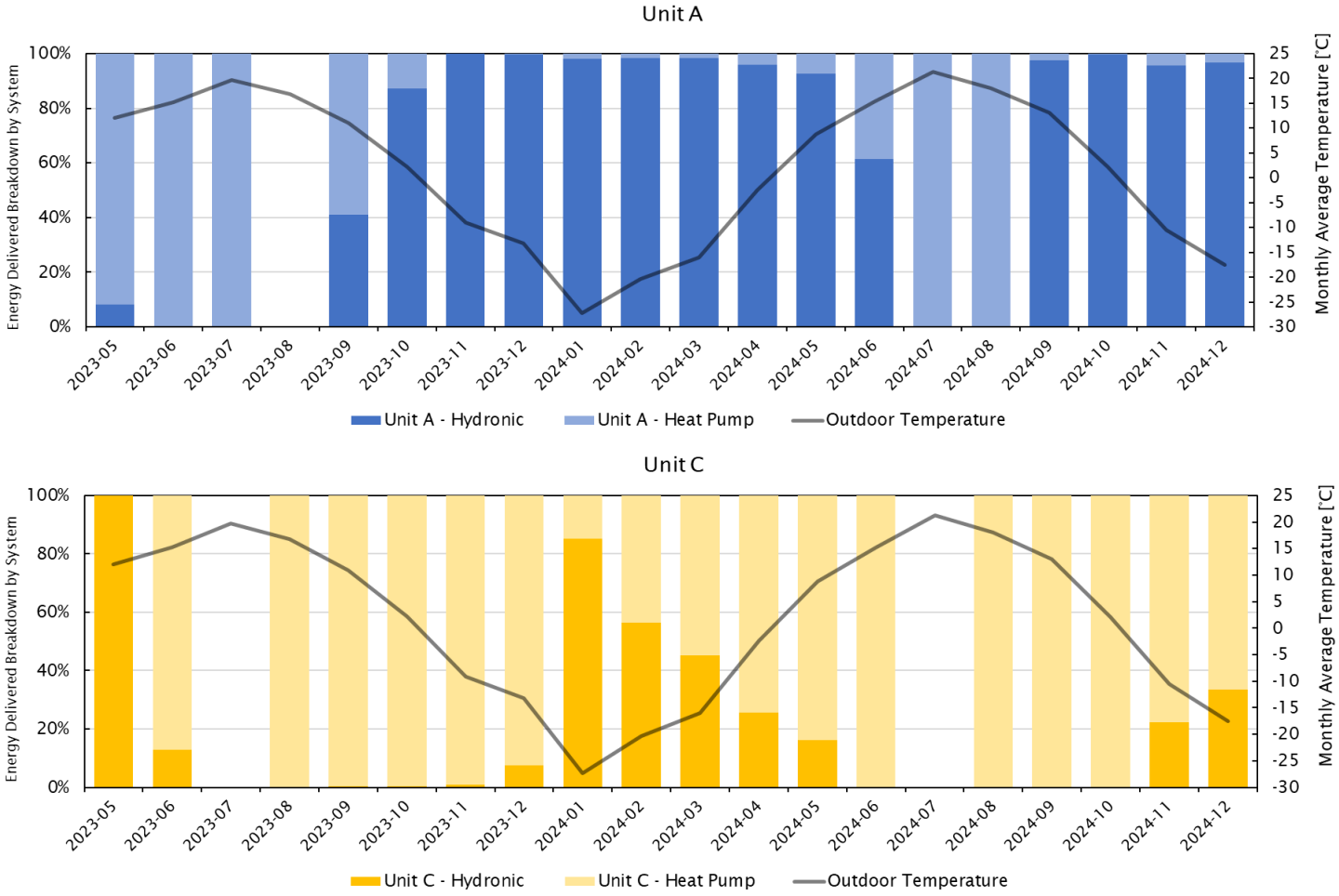


*Figure 3.13 – Monthly percent (%) breakdown of energy delivered by heat pump and hydronic system, normalized by the number of days in each month.*

## 3.4 Energy Savings, Cost Savings and GHG Emissions Reduction

Since utility data for individual units was not available, a simplified approach was used to estimate the theoretical energy savings from the heat pump retrofit over a typical meteorological year. Note that this analysis assumes typical oil boiler efficiency and does not account for heat recovery from in-suite HRVs. The key steps are:

1. Based on the monitoring data, a linear regression between the heat pump's energy output and outdoor temperature (in 1˚C bins) was conducted (dark blue line in Figures 3.14a and 3.15a). Similarly, a linear regression was conducted between the heat pump's electricity consumption and outdoor air temperature (light blue line in Figures 3.14a and 3.15a). The regressions were limited to an outdoor temperature range of -22˚C to 15˚C for Unit A, and -30˚C to 15˚C for Unit C, to reflect the observed operating ranges for heat pump heating. See Figure 3.2 for the outdoor temperature distribution of the monitoring data for each unit.
2. The theoretical baseline consumption of the boiler if the heat pump portion of heating was instead supplied by a boiler was estimated at each temperature by dividing the heat pump's energy output (fitted) by the oil boiler's rated efficiency, AFUE, of 0.85 (orange line in Figures 3.14a and 3.15a).
3. Based on the monitoring data, a linear regression between the hydronic baseboard heating output and outdoor temperature (in 1˚C bins) was conducted (dark green line in Figures 3.14b and 3.15b). The theoretical boiler consumption at each temperature was estimated by dividing the hydronic baseboard heating output (fitted) by the oil boiler's rated efficiency (AFUE = 0.85) to arrive at the light green line in Figures 3.14b and 3.15b.
4. To calculate the current (i.e. post-retrofit) total consumption (i.e. using a combination of heat pump and baseboard heating), the heat pump's electricity consumption (fitted) from Step 1, and boiler consumption for the hydronic heating (in ekWh) from Step 3 were summed. To illustrate this step in Figure 3.14c and Figure 3.15c, the light blue line and the light green line are summed to yield the purple line.
5. The theoretical baseline (i.e. pre-retrofit) total consumption (i.e. using hydronic baseboard heating only) was estimated by summing the theoretical baseline consumption of using baseboard to supply the heat pump portion of heating, from Step 2, and the boiler consumption from Step 3. To illustrate this step in Figure 3.14c and Figure 3.15c, the orange line and the light green line are summed to yield the red line.
6. Energy savings were calculated by subtracting the current total consumption from the baseline total consumption. To illustrate this step in Figure 3.14c and Figure 3.15c, energy savings are estimated as the red line minus the purple line.
7. The five-minute savings were multiplied by 12 to translate to hourly savings at a given outdoor temperature. Annual energy savings were determined by calculating the sum-product of the hourly energy savings (at varying outdoor temperatures) and the outdoor temperature distribution (in hours) of the Canadian Weather Year for Energy Calculation (CWEC) 2020 Version 2.0

Yellowknife weather file.[14] The outdoor temperature distribution is shown in Figure 3.16.

8. Greenhouse gas emissions from the current and the baseline total consumptions were calculated, using the emissions factor of 2.69 $kgCO_2e/L$ for oil #2 and 0.01966 $tCO_2e/MWh$ for electricity.[15] Emission reductions were estimated as the difference between the two cases.

9. Finally, the baseline total utility cost was calculated by multiplying the baseline total consumption by the cost for heating oil of $0.1303/ekWh.[16] The current total utility cost was calculated by multiplying the heat pump consumption by the electricity cost of $0.36/kWh,[17] plus the boiler consumption multiplied by the unit cost of heating oil. Cost savings were determined as the difference between the current and the baseline utility costs.

[14] Canadian Weather Year for Energy Calculation (CWEC) 2020 files are developed by NRCan for 564 locations (Yellowknife is one of these). Each CWEC file is created by joining twelve Typical Meteorological Months selected from a database of up to 20 years (1998-2017) of the Canadian Weather Energy and Engineering Datasets (CWEEDS) hourly data. This data file uses the most 'typical' months of weather data over the period. https://open.canada.ca/data/en/dataset/55438acb-aa67-407a-9fdb-1cb21eb24e28

[15] Provided by Arctic Energy Alliance; from AEA's Technical Standards.

[16] Based on the 5-year average price for residential heating oil of $1.39/L for Yellowknife, divided by the calorific value of 38.4 MJ/L for Oil #2 and multiplied by a conversion factor (3.6 MJ/kWh), to obtain the heating oil cost of $0.1303/ekWh. References: AEA's Fuel Cost Library (https://aea.nt.ca/resources/studies-and-reports/, revised April 2025) and AEA's Technical Standards.

[17] Published 5-year average electricity rate from AEA's Fuel Cost Library for Yellowknife (revised April 2025). AEA's Fuel Cost Library: https://aea.nt.ca/resources/studies-and-reports/

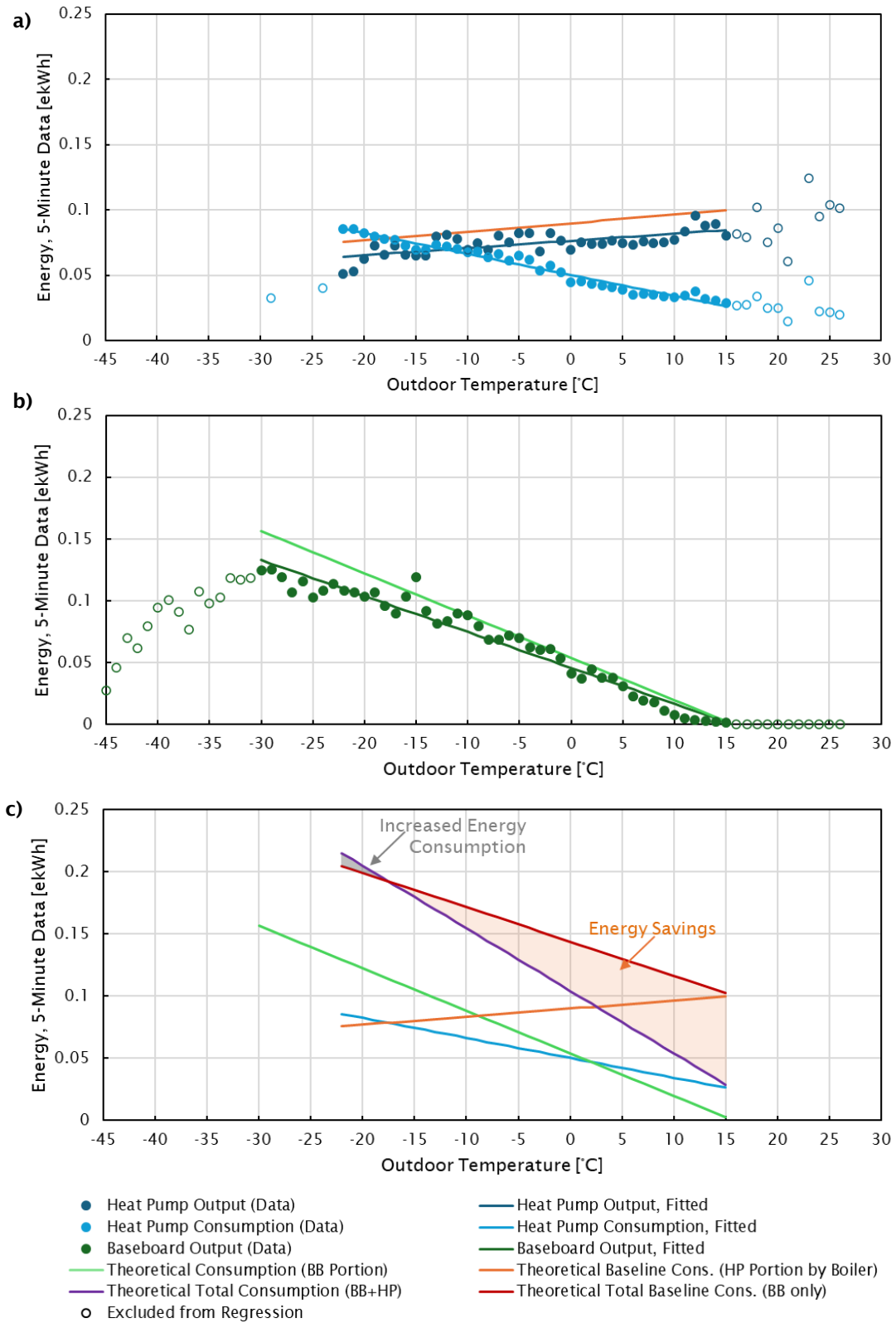


*Figure 3.14 – Determining the theoretical energy savings between current heating consumption (from heat pump and baseboard heating) and theoretical baseline consumption (baseboard only) for Unit A.*

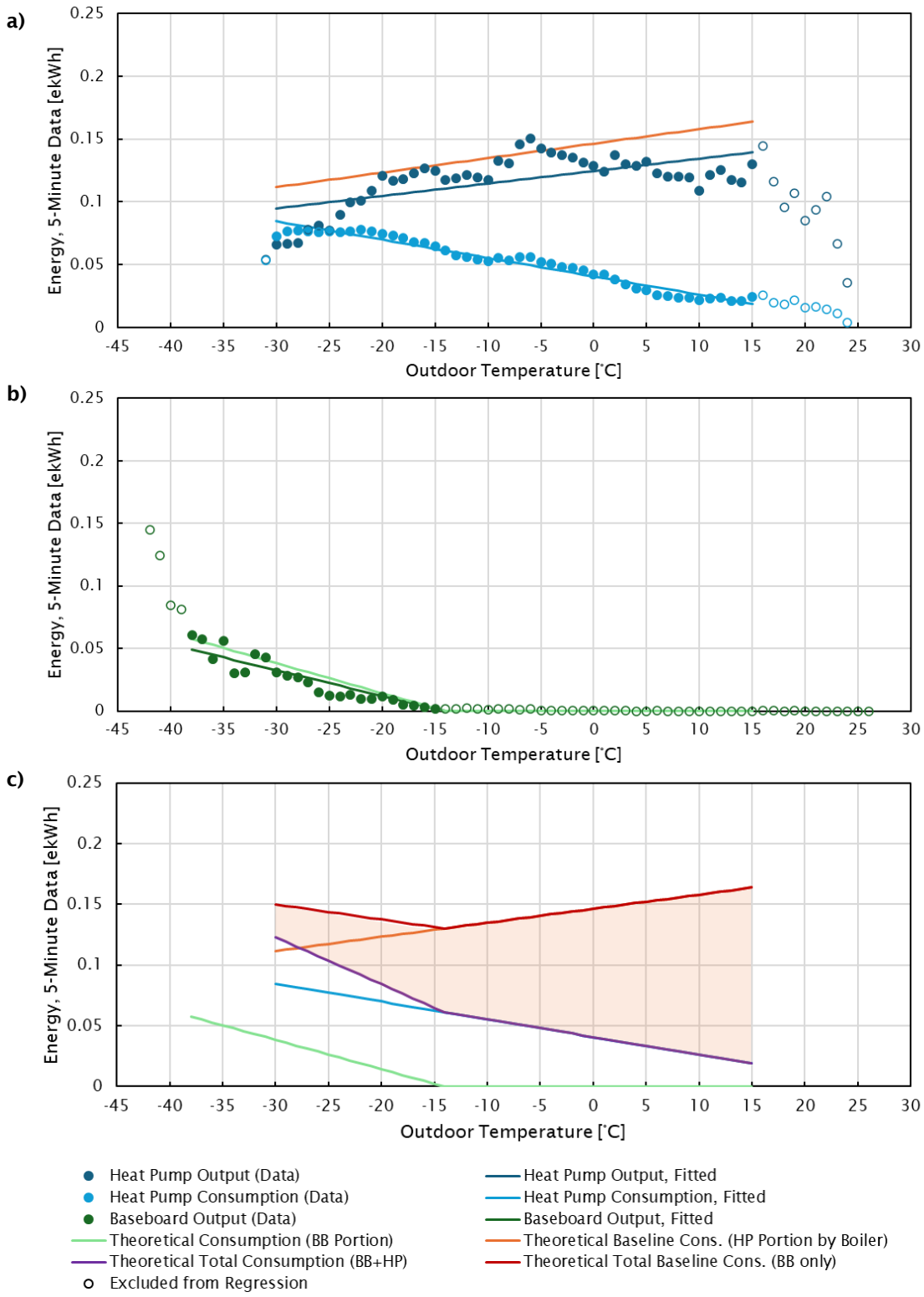


*Figure 3.15 – Determining the theoretical energy savings between current heating consumption (from heat pump and baseboard heating) and theoretical baseline consumption (baseboard only) for Unit C.*

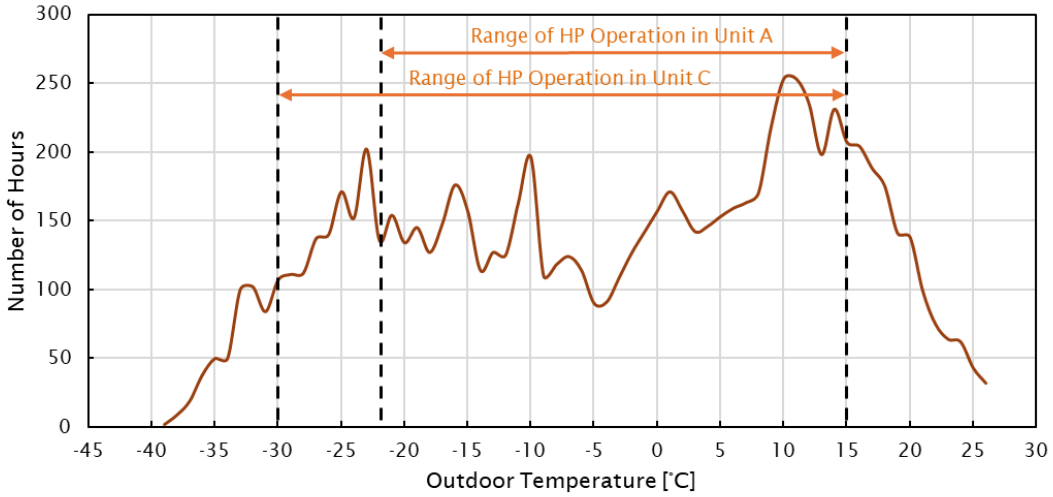


*Figure 3.16 – Outdoor air temperature distribution of the CWEC 2020v2 Yellowknife weather file.*

The resulting weather-normalized annual energy, emissions, and utility cost savings are summarized in Table 3.4. Note that the savings were calculated only over the range of outdoor temperatures observed during heat pump operation for each of Units A and C. Heat pump capacities at outdoor temperatures lower than those observed could not be confirmed, and thus were excluded from the analysis. Because the evaluated outdoor temperature ranges differ between Units A and C, the resulting savings should not be directly compared across the two units.

TABLE 3.4 ANNUAL ENERGY AND EMISSIONS SAVINGS PER HOME

| Unit Number | Energy Savings (ekWh/year) | GHG Emissions Savings ($kgCO_2e$) | Utility Cost Savings ($) |
|---|---|---|---|
| Unit A | 2,536 | 1,522 | ($541) |
| Unit C | 7,716 | 2,913 | $51 |

Both units demonstrated energy savings and emission reductions. Heating oil consumption from the baseline was replaced by electricity, which has a substantially lower emissions factor. As a result, both homes realized relatively greater emission reductions due to fuel switching and improved heat pump efficiency, compared to the energy savings attributable to heat pump efficiency alone. However, because electricity costs are nearly three times that of heating oil (on a per ekWh consumed basis), only Unit C (which was operating as anticipated) achieved utility cost savings, despite both units using less total combined energy after the heat pump retrofit.

# 4 Summary of Findings

This final report includes results from data collected between May 1, 2023, and December 31, 2024. In all, the results suggest that cold climate ductless air-source heat pumps have the potential to serve as the primary heating technology for heating in sub-arctic regions, as long as some form of supplemental heating can be provided during periods below the heat pump's rated outdoor operating conditions. Given the efficiencies exhibited in this study, utilizing heat pumps during shoulder seasons and during relatively milder winter conditions could maximize their potential, and reduce dependency on other fuel sources. However, it is important to note that the high cost of electricity in the Northwest Territories remains a concern. Proper sizing of equipment based on design heat loads and an optimized control strategy will also help ensure heat pumps operate to their full potential.

As discussed over the course of the project, the control strategy for Unit A was not being executed as intended, and it appears that the heat pump and the hydronic heating system were competing for a large portion of the heating season, which in turn negatively affected the performance of the heat pump. Another key finding was that the indoor unit filter in Unit A had not been cleaned regularly, which likely contributed to reduced system performance. In contrast, Unit C was missing its filter entirely. While this may have prevented shorter term performance issues related to airflow restriction in Unit C, it also means that there may be longer term performance issues, as this filter is intended to keep the coil/heat exchanger clean. These findings highlight the importance of adequate system commissioning/controls strategy and the importance of regular maintenance per manufacturer recommendations.

Extrapolating the measured data to associated energy, emissions, and cost savings, the performance of both Units A and C demonstrated that a cold climate heat pump with supplemental heating can achieve meaningful energy and emissions savings in northern climates. Unit C, which was operating as expected achieved utility cost savings. On the other hand, Unit A's results show how energy savings can be compromised when controls and maintenance are not optimized.

We trust that this document meets the intent of the final report. Please do not hesitate to contact us if you have any further questions.

Yours truly,

**Laura Simandl** | MS, P.Eng. (BC), P.E. (WA)
Project Engineer
lsimandl@rdh.com

Reviewed by

**Christy Love** | P.Eng (BC)
Principal, Senior Specialist
clove@rdh.com

**Samantha Chum** | MASc, CMVPIT
EIT 2
schum@rdh.com

**Jun Tatara** | Dipl.T.
Associate, Project Consultant
jtatara@rdh.com